

Long-distance continuous-variable quantum key distribution using separable Gaussian states

Jian Zhou¹, Duan Huang^{1,2}, and Ying Guo^{1*}

¹*School of Information Science and Engineering,
Central South University, Changsha 410083, China*

²*State Key Laboratory of Advanced Optical Communication Systems and Networks,
Department of Electronic Engineering, Shanghai Jiao Tong University, Shanghai 200240, PR China.*

(Dated: December 5, 2018)

Continuous-variable quantum key distribution (CVQKD) is considered to be an alternative to classical cryptography for secure communication. However, its transmission distance is restricted to metropolitan areas, given that it is affected by the channel excess noise and losses. In this paper, we present a scheme for implementing long-distance CVQKD using separable Gaussian states. This tunable QKD protocol requires separable Gaussian states, which are squeezed and displaced, along with the assistance of classical communication and available linear optics components. This protocol originates from the entanglement of one mode and the auxiliary mode used for distribution, which is first destroyed by local correlated noises and restored subsequently by the interference of the auxiliary mode with the second distant separable correlated mode. The displacement matrix is organized by two six-dimensional vectors and is finally fixed by the separability of the tripartite system. The separability between the ancilla and Alice and Bob's system mitigates the enemy's eavesdropping, leading to tolerating higher excess noise and achieving longer transmission distance.

I. INTRODUCTION

Quantum key distribution (QKD) [1, 2] enables two distant parties, conventionally called Alice and Bob, who have access to an authenticated classical channel, to share secret keys in the presence of eavesdropper, Eve. The unconditional security of an ideal QKD protocol has been established even if it is exposed to an adversary, who possesses unlimited computing power and technological capabilities [3–6]. Normally, QKD is divided into two kinds: discrete-variable (DV) QKD [2, 7], which relies on photon counting techniques, and continuous-variable (CV) QKD [8–11], which relies on coherent detection. Equipped with the decoy state technique [12], DVQKD can realize hundreds of kilometers of communication [13]. With the help of a satellite, the transmission distance of QKD has been extended to 1200 kilometers [14]. Another branch of QKD, CVQKD, which has stable, reliable light resources and high detection efficiency, is more compatible with classical optical communications when compared to DVQKD [9]. However, despite all the advantages, CVQKD cannot yet replace DVQKD since its transmission distance is too short [15, 16]. One reason for the short distance is the presence of the eavesdropper, Eve, who can perturb the quantum system using the most general strategies allowed by quantum mechanics. Another one is that CVQKD schemes require a far more complicated error correction procedure, which further restricts the secure transmission distance.

Einstein associated entanglement with spooky action-at-a-distance [17], which is different from the current view in quantum information theory that regards entanglement as a physical resource. Entanglement [18] has

been widely applied to QKD [19], quantum dense coding [20], quantum teleportation [21], entanglement swapping [22] and beating classical communication complexity bounds [23]. For example, global quantum operations can be implemented in quantum teleportation utilizing entanglement and classical communication. Great effort has been devoted to distributing and manipulating entanglement among separated parties. In addition, a scheme of entangling two distant parties based on communication via a quantum channel and local operations and classical communication (LOCC) was proposed [24]. Entanglement between distant parties can be created by sending a mediating particle between them via a quantum channel: swap the first particle with the ancilla, send it through the channel and entangle it with the second particle. Besides the qubit protocol, distributing CV entanglement by separable Gaussian states has also been suggested [25, 26]. Two separable modes A and B may be entangled after interacting with the auxiliary mode C . Unfortunately, pure quantum states cannot achieve this target. Moreover, Alice and Bob usually apply squeezing and displacement operations on these modes to enhance the practical quantum information processing. Recently, the aforementioned operations have been verified in experiment [27, 28].

To lengthen the transmission distance of the CVQKD system, we develop an improved protocol which transmits a separable ancilla without sending the secret information directly as usual. It may entangle mode A , in Alice's laboratory, with separable mode B , in Bob's distant laboratory, by sending an ancillary mode C which is separable from the subsystem (AB) [24]. Normally, the quantum transmission channel is assumed to be under Eve's control in QKD. We exemplify the entanglement between Alice's and Bob's modes and the separability between the ancilla and the kept particle by calculating the

* Corresponding author: guoyingcsu@sina.com

lowest eigenvalue. In previous fully Gaussian protocols, Eve's system E purifies AB , so that, $S(E) = S(AB)$. Fortunately, in this scheme, the transmitted particle C that may be attacked by Eve is separable from AB . The eavesdropper cannot get access to Alice's and Bob's laboratories as well as the information transmitted in the classical channel. In this case, it is impossible for the eavesdropper to recover the process of the protocol and hence she cannot extract any information. In such a scenario, the proposed scheme reduces the information leaked to the eavesdropper, thus enables longer transmission distance.

This paper is organized as follows: In Sec. II, we review the distribution of entanglement with separable states. In Sec. III, we present the details of CVQKD scheme with separable states. Sec. IV shows the performance of the proposed CVQKD scheme under general eavesdropping. Finally, we conclude this paper in Sec. V.

II. ENTANGLEMENT DISTRIBUTION WITH SEPARABLE STATES

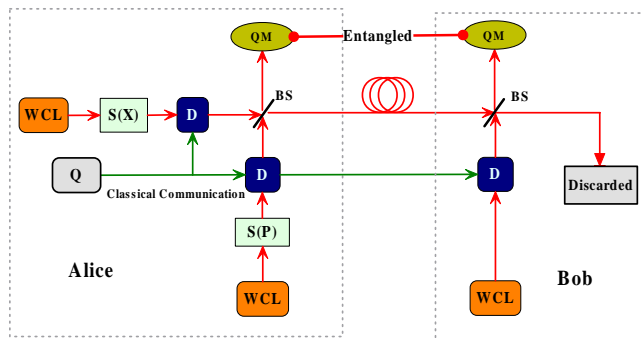


FIG. 1. (Color online) Alice's particle and Bob's particle interact with a mediating particle C continuously. Alice and Bob get entangled while leaving C separable from the system AB . WCL denotes weak coherent laser, and $S(X)$, $S(P)$ are compression operations on along position and momentum directions. D is a local displacement distributed according to the Gaussian distribution with correlation matrix Q .

Distributing entanglement with separable states is a breakthrough in the theory of quantum entanglement. It has been shown that separable Gaussian states can be used for implementing entanglement distribution [25, 26]. As shown in Fig. 1, this process can be accomplished by communication via a quantum channel and LOCC.

At the start of the original entanglement distribution protocol, Alice prepares systems A and C in a Gaussian state while Bob prepares system B in a Gaussian state. The three quantum systems are fully separable at this stage. Alice squeezes her two systems: one along the position quadrature and the other along the momentum quadrature. In order to keep the ancilla separable from system AB , a displacement operation is applied to each

of the three systems. Note that the displacement is dependent on the squeezing parameters r_1 and r_2 . Alice sends her two systems into a beam splitter. The beam splitter operation on modes A and C results in a state separable with respect to two bipartitions: $B - AC$ and $C - AB$. One of the outputs is stored in Alice's quantum memory (QM). The other is sent to Bob via a quantum channel. Bob also applies a beam splitter operation on modes B and C . Mixing of modes B and C on a balanced beam splitter finally entangles A and B while C still remains separable from AB .

In what follows, we recall how a displacement operation may make the transmitted ancilla C separable from AB [25]. Before the displacement operation, modes A and C are in a two-mode squeezed vacuum state and mode B is in a vacuum state. The output of the first beam splitter is a two-mode squeezed vacuum state with the following covariance matrix (CM):

$$\gamma_{AC} = \begin{bmatrix} \cosh(2\tau)I_2 & \sinh(2\tau)\sigma_z \\ \sinh(2\tau)\sigma_z & \cosh(2\tau)I_2 \end{bmatrix}, \quad (1)$$

where $\tau \geq 0$ is the squeezing parameter. Modes A and C are entangled when the lower symplectic eigenvalue ν_{\min} of the partial transpose of CM γ_{AC} is less than one [25]. The CM of the three-mode system ABC is given by

$$\gamma_{ABC} = \begin{bmatrix} \cosh(2\tau)I_2 & 0 & \sinh(2\tau)\sigma_z \\ 0 & I_2 & 0 \\ \sinh(2\tau)\sigma_z & 0 & \cosh(2\tau)I_2 \end{bmatrix}. \quad (2)$$

We add an excess non-negative matrix P to γ_{ABC}

$$\gamma_{ABC}^1 = \gamma_{ABC} + xP, \quad (3)$$

to entangle mode A and modes BC , while leaving the other two bipartitions separable. We follow the method for the construction of three-mode entangled Gaussian states in [29] to build matrix P . The entanglement between modes A and C can be destroyed by adding a positive multiple of sum of the projectors onto the subspace spanned by two six-dimensional vectors [25, 29]. The negative eigenvalue of the CM is $\lambda = -(1 - e^{-2\tau})$ with its eigenvector $p_\lambda = p_1 + ip_2$ for $p_1 = (0, 1, 0, 1)^T$ and $p_2 = (1, 0, -1, 0)^T$. We extend p_1 and p_2 to the six-dimensional vectors $q_1 = (0, 1, 0, -2, 0, 1)^T$ and $q_2 = (1, 0, 2, 0, -1, 0)^T$ with the displacement matrix $P = q_1 q_1^T + q_2 q_2^T$. In order to smear the entanglement between modes A and C , we add a sufficiently large, non-negative multiple xP to the CM as shown in Eq. (3) and obtain

$$\gamma_{ABC}^1 = \begin{bmatrix} aI_2 & 2x\sigma_z & b\sigma_z \\ 2x\sigma_z & (1+4x)I_2 & -2xI_2 \\ b\sigma_z & -2xI_2 & aI_2 \end{bmatrix}. \quad (4)$$

where $a = \cosh(2t) + x$ and $b = \sinh(2t) - x$. Then the lowest symplectic eigenvalue of matrix $(\gamma_{ABC}^1)^{(T_C)}$ can be derived as [30],

$$\nu_{\min} = \frac{\sqrt{(1+6x+e^{-2\tau})^2 - 32x^2} - (1+2x-e^{-2\tau})}{2}. \quad (5)$$

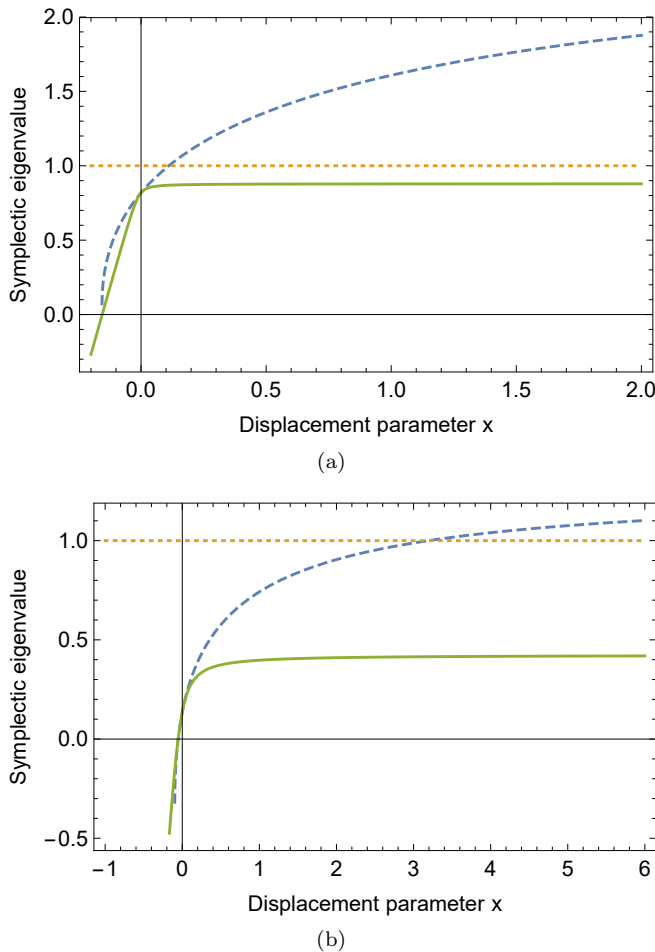


FIG. 2. The eigenvalues, ν_{\min} and κ_{\min} , as a function displacement parameter x , for different compression parameters τ , correspond to the dashed and full lines. The compression parameter $\tau = 0.1$ in (a) and $\tau = 1$ in (b). The dotted lines denote the boundary of separability.

The separable bound of C and AB is $\frac{e^{2\tau}-1}{2}$, where the parameter x should be equal or greater than this value. On the other hand, the lowest eigenvalue of matrix $(\gamma_{ABC}^1)^{(T_A)}$ can be calculated as

$$\kappa_{\min} = \frac{1 + 6x + e^{-2\tau} - \sqrt{(1 + 2x - e^{2\tau})^2 + 32x^2}}{2}. \quad (6)$$

Taking $x \geq 0$ and $\tau \geq 0$ in Eq. 6, the lowest eigenvalue is less than one, which verifies that there is entanglement between A and BC . Fig. 2 shows the lowest symplectic eigenvalue of matrix $(\gamma_{ABC}^1)^{(T_C)}$ and $(\gamma_{ABC}^1)^{(T_A)}$. To satisfy the separability of $C - AB$, the lowest symplectic eigenvalue corresponding to the dashed line should be greater than one. Similarly, the lowest symplectic eigenvalue corresponding to the full line ought to be less than one to ensure the entanglement between A and BC . Finally, after applying reverse operation of the beam splitter on γ_{ABC}^1 , the covariance matrix of the random displacement distributed according to Gaussian distribution

is fixed. The beam splitter transforms the CM in (4) to CM γ_{ABC}^2 that is as follow:

$$\gamma_{ABC}^2 = \begin{bmatrix} aI_2 & \frac{2x+b}{\sqrt{2}}\sigma_z & \frac{2x-b}{\sqrt{2}}\sigma_z \\ \frac{2x+b}{\sqrt{2}}\sigma_z & \frac{1+a}{2}I_2 & \frac{1+4x-a}{2}I_2 \\ \frac{2x-b}{\sqrt{2}}\sigma_z & \frac{1+4x-a}{2}I_2 & \frac{1+8x+a}{2}I_2 \end{bmatrix}. \quad (7)$$

The symplectic eigenvalue of CM γ_{AB} can be calculated as $\nu = 0.3968$ for $e^{2\tau} = 10$, and the entanglement can be obtained as $E_N = -\log_2 \nu \approx 1.33$ ebits.

According to the entanglement distribution with separable Gaussian states, we find that the entanglement is firstly destroyed by displacement operations, which makes the auxiliary mode separable from sender's mode. After that, the auxiliary mode is sent to Bob who partially restores the entanglement by mixing it with his suitably classically correlated mode, leading to the entanglement enhancement. Using this elegant characteristics, we propose an improved CVQKD scheme to lengthen the maximum transmission distance with separable Gaussian states.

III. CONTINUOUS VARIABLE QUANTUM KEY DISTRIBUTION WITH SEPARABLE GAUSSIAN STATES

This section is divided into three parts: the first part gives the CVQKD protocol using separable Gaussian states, the second part analyses the security of normal CVQKD protocol, while the third subsection states the merit of the protocol based on separable Gaussian states.

A. Design of the CVQKD protocol using separable Gaussian states

Two normal parties, Alice and Bob aim to share secret key. For the sake of simplifying the process, we add the displacement operation in the form of matrix while the practical displacement is not complex. The prepare and measure description of the CVQKD based on entanglement distribution protocol using Gaussian states is shown in Fig. 3 and is described as follows.

- Alice prepares two squeezed vacuum states which are position-squeezed and momentum-squeezed vacuum states, respectively. Displacement operations are added on these squeezed states. The output of the first beam splitter is a two-mode squeezed vacuum state if we ignore the displacement operation.
- Alice detects one of the outputs with homodyne detection and sends another one to Bob via a quantum channel.
- After receiving Alice's mode, Bob interferes his vacuum state with the received state at a balanced beam splitter.

- Bob heterodynes one of the beam splitter's outputs with the self-referenced strategy, whereas another one is discarded directly.

In Alice's laboratory, she prepares two states, one position-squeezed vacuum state and one momentum-squeezed vacuum state given by

$$\gamma_A = \begin{bmatrix} e^{2\tau} & 0 \\ 0 & e^{-2\tau} \end{bmatrix}, \quad \gamma_C = \begin{bmatrix} e^{-2\tau} & 0 \\ 0 & e^{2\tau} \end{bmatrix}. \quad (8)$$

The CM of the beam splitter's output can be expressed as

$$\gamma_{AC} = \begin{bmatrix} VI_2 & \sqrt{V^2-1}\sigma_z \\ \sqrt{V^2-1}\sigma_z & VI_2 \end{bmatrix}, \quad (9)$$

with $V = \frac{e^{2\tau}+e^{-2\tau}}{2}$, $\sigma_z = \begin{bmatrix} 1 & 0 \\ 0 & -1 \end{bmatrix}$ and $I_2 = \begin{bmatrix} 1 & 0 \\ 0 & 1 \end{bmatrix}$. The CM of ABC before transmission without displacement is

$$\gamma_1 = \begin{bmatrix} VI_2 & 0 & \sqrt{V^2-1}\sigma_z \\ 0 & I_2 & 0 \\ \sqrt{V^2-1}\sigma_z & 0 & VI_2 \end{bmatrix}. \quad (10)$$

Taking the displacement into consideration, the corresponding CM becomes

$$\gamma_2 = \begin{bmatrix} aI_2 & b\sigma_z & 2x\sigma_z \\ b\sigma_z & aI_2 & -2xI_2 \\ 2x\sigma_z & -2xI_2 & (1+4x)I_2 \end{bmatrix}, \quad (11)$$

with $a = V+x$ and $b = \sqrt{V^2-1}-x$. The linear channel can be equivalent to a beam splitter with transmittance η , the function of transmission distance $\eta = 10^{-\frac{L}{50}}$. The equivalent CM of the channel is

$$B_\eta = \begin{bmatrix} I_2 & 0 & 0 & 0 \\ 0 & I_2 & 0 & 0 \\ 0 & 0 & \sqrt{\eta}I_2 & \sqrt{1-\eta}I_2 \\ 0 & 0 & -\sqrt{1-\eta}I_2 & \sqrt{\eta}I_2 \end{bmatrix}. \quad (12)$$

After the attenuation of the channel, the CM of the whole system ABC becomes

$$\gamma_3 = \begin{bmatrix} aI_2 & b\sqrt{\eta}\sigma_z & 2x\sigma_z \\ b\sqrt{\eta}\sigma_z & (a\eta + (1-\eta)N_0)I_2 & -2x\sqrt{\eta}I_2 \\ 2x\sigma_z & -2x\sqrt{\eta}I_2 & (1+4x)I_2 \end{bmatrix}, \quad (13)$$

where N_0 is the variance of channel thermal noise. In normal QKD protocols, Bob performs homodyne or heterodyne detection on the received signals. However, the direct-detection scheme may leave the attacker loophole to eavesdrop information. Instead, Bob prepares a vacuum state and applies a displacement operation on it. Using a balanced beam splitter, Bob mixes the incoming mode with his own mode. The second balanced beam splitter transforms the CM into $\gamma_4 = B_{BC} \cdot \gamma_3 \cdot B_{BC}^T$. After the beam splitter, one of the outputs is detected

with homodyne detection using the self-reference technique, while another one is discarded directly. The CM of the system AB is

$$\gamma_{AB} = \begin{bmatrix} aI_2 & \frac{2x+b\sqrt{\eta}}{\sqrt{2}}\sigma_z \\ \frac{2x+b\sqrt{\eta}}{\sqrt{2}}\sigma_z & \frac{1+N_0+4x(1-\sqrt{\eta})+a\eta-N_0\eta}{2} \end{bmatrix}, \quad (14)$$

which can be used for calculating the secret key rate of the protocol.

B. Attacking strategy with general eavesdropping

A QKD protocol is secure against general attack when it is secure against Gaussian collective attack [4, 5]. This part performs an asymptotic security analysis based on infinitely-many uses of the channel under Gaussian collective attack. In each transmission, Eve may intercept the mode and make it interact with an ensemble of ancillary vacuum modes via a general unitary operation. One of the output modes is sent to Bob while another one is stored in Eve's quantum memory (QM). These states in QM will be measured at the end of the protocol collectively. Taking reverse reconciliation into account, the final key rate can be derived as

$$R = \xi I_{AB} - \chi_{BE}, \quad (15)$$

where ξ denotes the reconciliation efficiency. We can compute the mutual information in terms of signal-to-noise ratio as

$$I_{AB} = \log_2 \frac{\varphi + 1}{\omega}. \quad (16)$$

φ is the modulation variance in shot-noise units and ω represents the equivalent noise. In the previous CVQKD protocols, Eve's system E purifies AB , so that $S(E) = S(AB)$, and $S(AB)$ can be calculated from the symplectic eigenvalues of the covariance matrix V_{AB} . In order to calculate the Holevo bound between Alice and Bob with the simplification of the expression, we denote the CM of the reduced state of systems AB as [31]

$$\gamma_{AB} = \begin{bmatrix} aI_2 & c\sigma_z \\ c\sigma_z & bI_2 \end{bmatrix}. \quad (17)$$

The symplectic eigenvalues can be calculated as [32]

$$\nu_{1,2}^2 = \frac{1}{2}[\Delta \pm \sqrt{\Delta^2 - 4D^2}], \quad (18)$$

where $\Delta = a^2 + b^2 - 2c^2$ and $D = ab - c^2$. Moreover, the symplectic eigenvalue of the conditional CM $V_{B|A}$ is $\nu_3^2 = b(b - c^2/a)$. Therefore, we have $S(AB) = G(\nu_1) + G(\nu_2)$ and $S(B|A) = G(\nu_3)$ with

$$G(x) = \left(\frac{x+1}{2}\right) \log_2 \left(\frac{x+1}{2}\right) - \left(\frac{x-1}{2}\right) \log_2 \left(\frac{x-1}{2}\right). \quad (19)$$

Consequently, the information eavesdropped by Eve can be bounded by $\chi_{BE} = S(AB) - S(B|A)$.

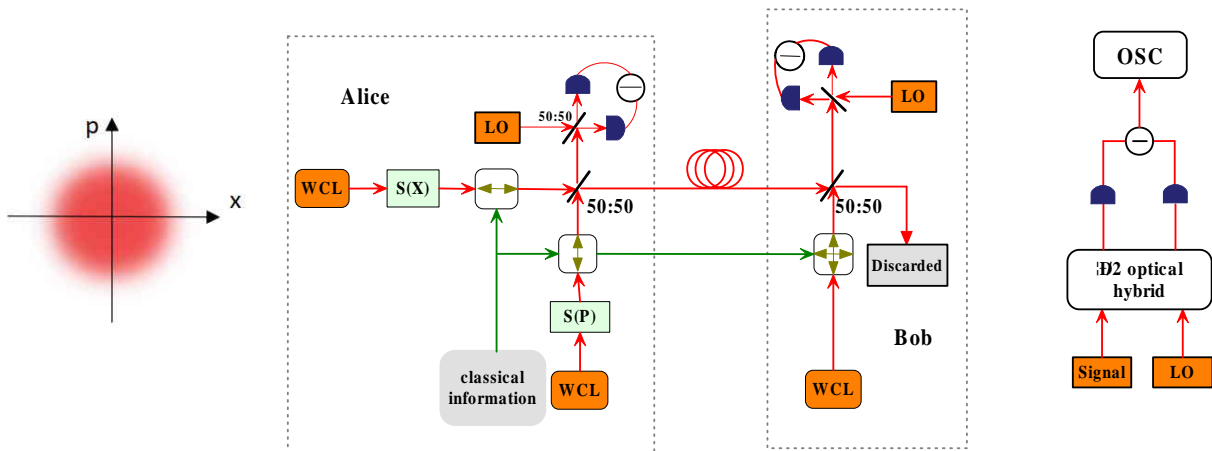


FIG. 3. (Color online) Scheme of CVQKD by sending separable Gaussian states. Alice and Bob apply displacement operation on their state at the stage of preparation. The displacement ensures the separability between C and AB . These modes emerge randomly in phase space obey Gaussian distribution as shown in the left part. The right part gives the detection scheme. WCL denotes weak coherent laser, and $S(X)$, $S(P)$ are compression operations along momentum and position directions. Double-headed arrow is local displacement distributed according to the correlation matrix.

C. Secret key rate of the separable-state CVQKD

It is necessary to note that the proposed protocol is different from the traditional protocol as the above-involved states are displaced before being mixed on the beam splitter. Without the displacement, the output of the first beam splitter is equivalent to a two-mode squeezed vacuum state. Another difference from the entanglement-based scheme is that Bob injects the received mode and his own mode into one beam splitter instead of performing homodyne or heterodyne detection directly. As analyzed in Sec. II, all these efforts are to keep the ancillary mode separable from system AB while completing the task of distribution entanglement between Alice and Bob. Whereas, in the traditional CVQKD system, the information is encoded on the mode that is sent to the channel under Eve's control. Eve may hide her attack in the channel noise. It has been assumed that Eve's system purifies AB , which implies that $S(E) = S(AB)$.

In the proposed protocol, the auxiliary mode used for distributing information is separable from AB . Alice's and Bob's labs as well as the classical communication are out of Eve's touch. Namely, Eve cannot steal any information by attacking the ancilla, leading to $S_E = 0$. A problem about upper bound arises. In [33–35], it has been proved that the secret key rate cannot be unbounded with increasing signal energy for normal CVQKD protocol [8]. The secret key rate satisfying the condition

$$R \leq I_{AB} - \chi_{BE} \leq G(\varphi) - G(\nu_1) - G(\nu_2). \quad (20)$$

The limit for $\varphi \rightarrow +\infty$ for the right part of the inequation is regular and finite [33–35]. The secret key rate will not be unbounded with increasing signal energy even though χ_{BE} is removed. A positive multiple of sum of the projectors is added to smear the entanglement between the

C and AB before transmission. The displacement which is proportional to the modulation variance also appears in the noise. The secret key rate of this scheme will not be unbounded as the signal-to-noise ratio is bounded regardless of the increasing signal energy. The advantage of keeping the ancillary state separable is the displacement before beam splitter. Bob uses a displaced state to interact with the ancilla rather than detects it directly. This operation is just to cut off Eve's disturbance. Then the secret key rate can be expressed as $R = \xi I_{AB}$, where ξ is the negotiation efficiency and I_{AB} can be calculated from the CM of system AB in Eq. (14).

IV. SIMULATION RESULTS

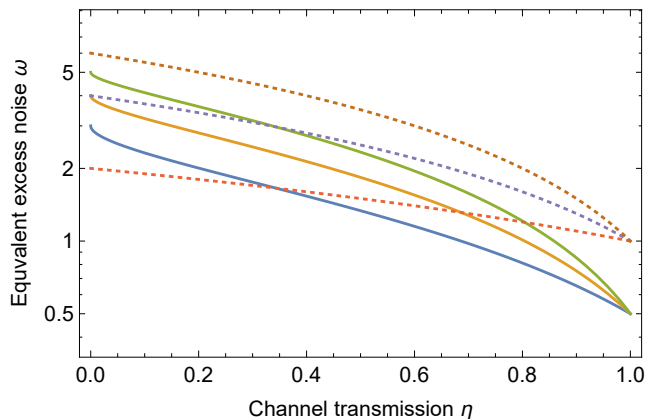


FIG. 4. (Color online) Equivalent excess noise as a function of channel transmission η . The dashed lines are the equivalent excess noise of original protocol while the full lines denote the proposed one. From bottom to top, $N_0 = 1, 3, 5$.

As discussed above, Alice and Bob can get the reduced CM γ_{AB} , from which they can calculate the secret key rate R in Eq.(15). Based on the Eq. (14), the equivalent excess noise can be expressed as

$$\omega = \frac{1 + (1 - \eta)N_0 + 4x(2 - \sqrt{\eta})}{2}, \quad (21)$$

which is plotted in Fig. 4. Compared with the traditional CVQKD protocol, the proposed protocol has an extra noise that is caused by the displacement operation. The displacement may decrease the key rate I_{AB} . Fortunately, it can also remove the entanglement between the ancillary particle and the kept particles.

To demonstrate the performance of the protocol, we consider both direct reconciliation and reverse reconciliation. In Fig. 5, we show the secret key rate of the

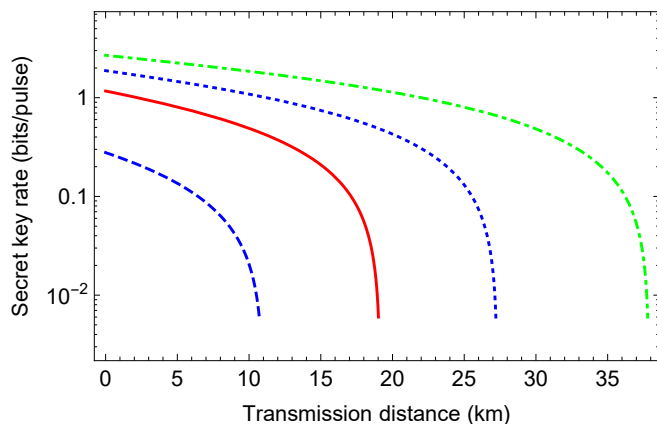


FIG. 5. (Color online) Secret key rates versus transmission distance from Alice to Bob of the direct reconciliation case. The secret key rate decreases as the grow of the transmission distance. Simulation results refer to $V = 2$ (blue dashed line), $V = 10$ (red full line), $V = 30$ (blue dashed line) and $V = 100$ (green dot-dashed line).

proposed protocol with direct reconciliation. From top to bottom, the dashed, full, dotted and dot-dashed lines refer to the modulation variances 2, 10, 30 and 100, respectively. With current technology, the 15dB squeezed states of light has already been detected in [36]. The transmission can exceed 15km, which corresponds to the 3dB restriction in direct reconciliation. Moreover, the excess noise has been taken into consideration with $\epsilon = 0.05$ and reconciliation efficiency is set $\beta = 0.95$ for all numerical simulations.

The simulation result in Fig. 6 is the secret key rate of the direct reconciliation case. The difference between thin lines and thick lines shows that modulation variance plays a positive role in the secret key rate. However, the displacement term limits the continued increase of the secret key rate. The full line, dot-dashed line and dotted line show channel noise has a negative effect on the secret key rate. We find that there is little effect of the noise on the secret key rate of the CVQKD system when the transmittance approaches to one.

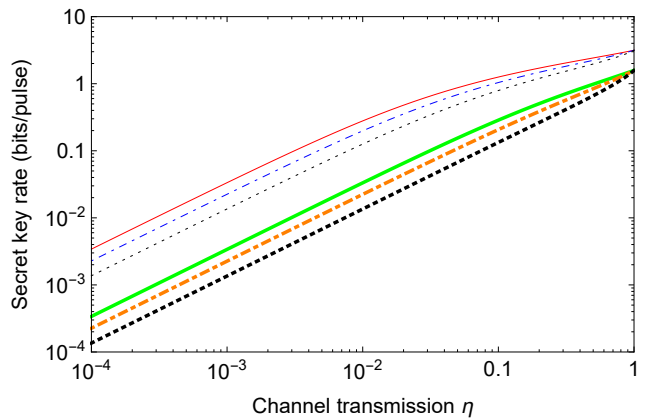


FIG. 6. (Color online) Secret key rates versus channel transmission, η . The full lines are under the ideal condition with zero excess noise while the dot-dashed and dotted lines correspond to $N_0 = 2$ and 4, respectively. The thick and thin lines are under the condition that modulation variance $V = 10$ and 100.

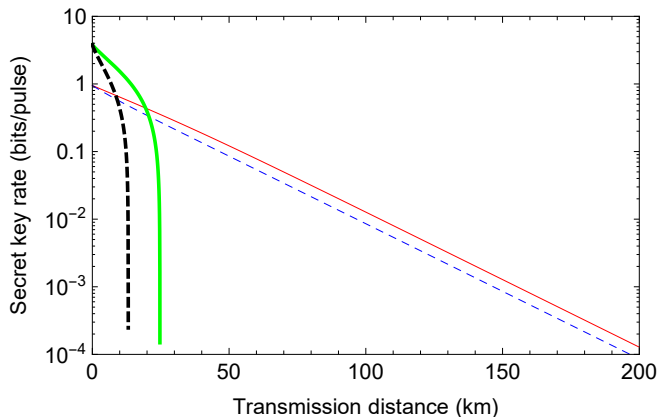


FIG. 7. (Color online) Secret key rates versus transmission distance, L . The full lines correspond to the condition with excess noise $N_0 = 1.01$ while the dashed lines correspond to $N_0 = 2$. The thin lines represent the proposed protocol with separable Gaussian states while the thick lines are the traditional protocols. In the simulation, the modulation variance $V = 30$.

Fig. 7 demonstrates the secret key rates of the proposed protocol using a separable ancilla in the reverse reconciliation case. The traditional CVQKD system can only transmit 30km due to the existence of the eavesdropper, whereas the proposed protocol achieves the transmission distance 200km at rate of 10^{-4} bits per pulse. The transmission distance of the separable-state CVQKD protocol is lower than that of the traditional one. This phenomenon may result from the abandon of the ancillary particle. Moreover, we can also find that the protocol has a better tolerance to noise than the traditional one.

In Fig. 8, we make a comparison between the secret key rate of our protocol and the fundamental limit [35, 37]. [35] proved the PLOB bound, while [34] later discussed

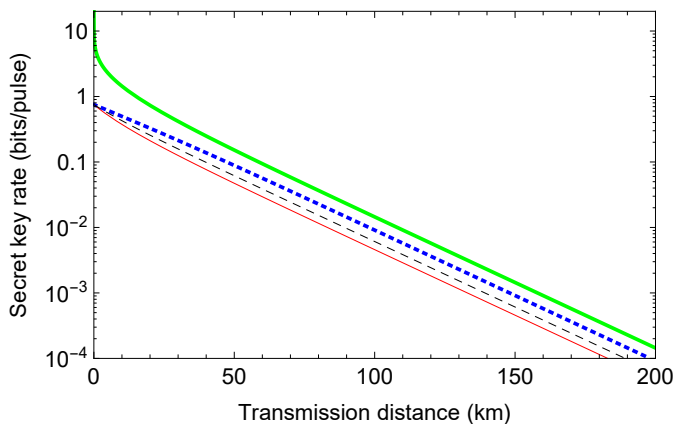


FIG. 8. (Color online) Secret key rates of CVQKD with separable states versus the upper bound of CVQKD. The thick green line is the upper bound of the traditional CVQKD. The dotted, dashed and thin full lines are the proposed CVQKD protocols with $N_0 = 1, 2, 3$, respectively.

the strong convergence of this bound. The top green line is the fundamental limit of general CVQKD protocol, which is given by $-\log_2(1 - \eta)$. η is channel transmittance of the pure-loss channel. As shown in [34, 35], the protocols whose secret key rate is based on the lower bound cannot come up with the upper bound when the transmittance η is less than 0.7. The protocol based on transmission of separable Gaussian states via a quantum channel and LOCC operation has a good performance on the aspect of transmission distance. This scheme has a good tolerance for excess noise and the transmission distance achieves 200km.

V. CONCLUSION

We have proposed an improved continuous-variable quantum key distribution protocol that is immune to

Eve's attack. This separable-state CVQKD protocol is different from the traditional protocol because the ancillary particle is separable from Alice and Bob's system. In previous protocols, the information is encoded on the particles which will pass through a quantum channel controlled by Eve. Eve can purify the whole system and extract as much information as the Holevo bound of the system. In addition, after the two respective particles interact continuously with an ancilla, they get entangled, leaving the ancilla separable all the time. The displacement operation in the preparation course plays a crucial role in smearing the entanglement between the ancilla and Alice and Bob's system. The secret key rate of the separable-state CVQKD will not be unbounded with increasing signal energy. The proposed protocol has good tolerance to extra noise and is able to keep abreast of the upper bound until 200km. We note that the proposed CVQKD protocol can be practically implemented using separable Gaussian states as entanglement preparation processes based on separable Gaussian states have been demonstrated in experiment [27, 28].

ACKNOWLEDGEMENTS

We would like to thank L. Mišta for helpful discussion. This work is supported by the National Natural Science Foundation of China (Grant Nos. 61572529) and the Fundamental Research Funds for the Central Universities of Central South University (2017zzts144).

-
- [1] H. Bennett Ch and G. Brassard, in *Conf. on Computers, Systems and Signal Processing (Bangalore, India, Dec. 1984)* (1984) pp. 175–9.
 - [2] A. K. Ekert, *Phys. Rev. Lett.* **67**, 661 (1991).
 - [3] D. Mayers, *Journal of the Acm* **48**, 351 (2001).
 - [4] A. Leverrier, *Phys. Rev. Lett.* **114**, 070501 (2015).
 - [5] A. Leverrier, *Physical Review Letters* **118**, 200501 (2017).
 - [6] V. Scarani, H. Bechmann-Pasquinucci, N. J. Cerf, M. Dušek, N. Lütkenhaus, and M. Peev, *Rev. Mod. Phys.* **81**, 1301 (2009).
 - [7] A. Acín, N. Gisin, and V. Scarani, *Phys. Rev. A* **69**, 012309 (2004).
 - [8] F. Grosshans and P. Grangier, *Phys. Rev. Lett.* **88**, 057902 (2002).
 - [9] C. Weedbrook, S. Pirandola, R. García-Patrón, N. J. Cerf, T. C. Ralph, J. H. Shapiro, and S. Lloyd, *Rev. Mod. Phys.* **84**, 621 (2012).
 - [10] Y. Guo, C. Xie, Q. Liao, W. Zhao, G. Zeng, and D. Huang, *Phys. Rev. A* **96**, 022320 (2017).
 - [11] Y. Guo, Q. Liao, D. Huang, and G. Zeng, *Phys. Rev. A* **95**, 042326 (2017).
 - [12] H.-K. Lo, X. Ma, and K. Chen, *Phys. Rev. Lett.* **94**, 230504 (2005).
 - [13] H.-L. Yin, T.-Y. Chen, Z.-W. Yu, H. Liu, L.-X. You, Y.-H. Zhou, S.-J. Chen, Y. Mao, M.-Q. Huang, W.-J. Zhang, H. Chen, M. J. Li, D. Nolan, F. Zhou, X. Jiang, Z. Wang, Q. Zhang, X.-B. Wang, and J.-W. Pan, *Phys. Rev. Lett.* **117**, 190501 (2016).
 - [14] S. K. Liao, W. Q. Cai, W. Y. Liu, L. Zhang, Y. Li, J. G. Ren, J. Yin, Q. Shen, Y. Cao, and Z. P. Li, *Nature* **549**, 43 (2017).
 - [15] S. Pirandola, C. Ottaviani, G. Spedalieri, C. Weedbrook, S. L. Braunstein, S. Lloyd, T. Gehring, C. S. Jacobsen,

- and U. L. Andersen, *Nature Photonics* **9**, 397 (2015).
- [16] Y. Wu, J. Zhou, X. Gong, Y. Guo, Z.-M. Zhang, and G. He, *Phys. Rev. A* **93**, 022325 (2016).
- [17] A. Einstein, B. Podolsky, and N. Rosen, *Phys. Rev.* **47**, 777 (1935).
- [18] R. Horodecki, P. Horodecki, M. Horodecki, and K. Horodecki, *Rev. Mod. Phys.* **81**, 865 (2009).
- [19] M. Epping, H. Kampermann, C. Macchiavello, and D. Brubß, *New Journal of Physics* **19** (2017).
- [20] T. Das, R. Prabhu, A. Sen(De), and U. Sen, *Phys. Rev. A* **92**, 052330 (2015).
- [21] J. G. Ren, P. Xu, H. L. Yong, L. Zhang, S. K. Liao, J. Yin, W. Y. Liu, W. Q. Cai, M. Yang, and L. Li, *Nature* **549**, 70 (2017).
- [22] P. Xu, H.-L. Yong, L.-K. Chen, C. Liu, T. Xiang, X.-C. Yao, H. Lu, Z.-D. Li, N.-L. Liu, L. Li, T. Yang, C.-Z. Peng, B. Zhao, Y.-A. Chen, and J.-W. Pan, *Phys. Rev. Lett.* **119**, 170502 (2017).
- [23] P. Trojek, C. Schmid, M. Bourennane, i. c. v. Brukner, M. Żukowski, and H. Weinfurter, *Phys. Rev. A* **72**, 050305 (2005).
- [24] T. S. Cubitt, F. Verstraete, W. Dür, and J. I. Cirac, *Phys. Rev. Lett.* **91**, 037902 (2003).
- [25] L. Mišta and N. Korolkova, *Phys. Rev. A* **77**, 050302 (2008).
- [26] L. Mišta and N. Korolkova, *Phys. Rev. A* **80**, 032310 (2009).
- [27] C. Peuntinger, V. Chille, L. Mišta, N. Korolkova, M. Förtsch, J. Korger, C. Marquardt, and G. Leuchs, *Phys. Rev. Lett.* **111**, 230506 (2013).
- [28] A. Fedrizzi, M. Zuppardo, G. G. Gillett, M. A. Broome, M. P. Almeida, M. Paternostro, A. G. White, and T. Paterek, *Phys. Rev. Lett.* **111**, 230504 (2013).
- [29] G. Giedke, B. Kraus, M. Lewenstein, and J. I. Cirac, *Phys. Rev. A* **64**, 052303 (2001).
- [30] G. Vidal and R. F. Werner, *Phys. Rev. A* **65**, 032314 (2002).
- [31] A. Holevo, *Probl. Inf. Transm.* **9**, 177 (1973).
- [32] A. Serafini, F. Illuminati, and S. De Siena, *Journal of Physics B* **37** (2004).
- [33] M. Takeoka, S. Guha, and M. M. Wilde, *Nature Communications* **5**, 5235 (2014).
- [34] M. M. Wilde, M. Tomamichel, and M. Berta, *IEEE Transactions on Information Theory* **63**, 1792 (2017).
- [35] S. Pirandola, R. Laurenza, C. Ottaviani, and L. Banchi, *Nature Communications* **8**, 15043 (2017).
- [36] H. Vahlbruch, M. Mehmet, K. Danzmann, and R. Schnabel, *Phys. Rev. Lett.* **117**, 110801 (2016).
- [37] S. Pirandola, R. García-Patrón, S. L. Braunstein, and S. Lloyd, *Phys. Rev. Lett.* **102**, 050503 (2009).